Available online at www.sciencedirect.com
SCIENCE DIRECT
Applied Catalysis A: General 291 (2005) 126–135
APPLIED CATALYSIS A: GENERAL
www.elsevier.com/locate/apcata

Low-content gold-ceria catalysts for the water–gas shift and preferential CO oxidation reactions

Weiling Deng, Janice De Jesus, Howard Saltsburg, Maria Flytzani-Stephanopoulos *

Department of Chemical and Biological Engineering, Tufts University, Medford, MA 02155, USA

Received 25 November 2004; received in revised form 4 February 2005; accepted 4 February 2005
Available online 4 June 2005

Abstract

Low-content (<0.6 at.%) gold-ceria samples were prepared by one-pot synthesis by the urea gelation/co-precipitation method, and by sodium cyanide leaching of high-content (5 at.%) gold-ceria materials prepared by deposition–precipitation. These catalysts, containing cationic gold in ceria, are active for both the low-temperature water–gas shift (WGS) reaction and the preferential oxidation of CO (PROX). The surface oxygen of ceria, as estimated by H_2-TPR, was used to normalize the WGS reaction rates. Cyclic temperature-programmed reduction with intermittent reoxidation showed that the surface structures of gold-ceria catalysts are highly reversible. Considerable reoxidation by oxygen or H_2O can occur even at ambient conditions. The stability of low-content gold-ceria catalysts for the PROX reaction in a realistic fuel gas mixture containing 1% CO–0.5% O_2–50% H_2–10% H_2O–15% CO_2–He was excellent. No drop in activity or selectivity was found in cyclic operation up to 150 °C.

Keywords: Gold; Cerium oxide; Water–gas shift; Selective CO oxidation; Temperature-programmed reduction; Redox; Fuel cells; Preferential oxidation of carbon monoxide

1. Introduction

Fuel cells are currently under intense development for both stationary and mobile applications. Fuel reforming is the practical method used to generate hydrogen for fuel cell power production. In the case of low-temperature PEM fuel cells, the hydrogen-rich gas requires further processing to remove or convert carbon monoxide, which poisons the electrocatalyst of the fuel cell anode. Catalytic conversion of CO takes place in two steps: first, the water–gas shift (WGS) reaction is used to reduce the CO concentration from 10–15 to ~1%, then preferential oxidation of CO (PROX) takes over to further reduce the CO concentration to below 50 ppm, which can be tolerated by PEM fuel cells. Highly active, stable, and selective catalysts are required for both the WGS and PROX reactions. The commercially used WGS catalyst in chemical plants, Cu–ZnO [1], is unsuitable for fuel cell application due to its sensitivity to temperature excursions, air exposure (pyrophoric), and water condensation during shutdown.

The catalysts examined more extensively for the conversion of CO via the WGS and the PROX reactions are the Pt-group metals supported on oxides, such as alumina, primarily for PROX [2–5], and ceria, primarily for the WGS reaction [6–8]. Ceria-supported platinum or iridium catalysts were found good for the removal of CO in the presence of large quantities of H_2 via the PROX reaction [9]. However, in the presence of H_2O and CO_2, these catalysts were not selective enough to be acceptable for fuel cell applications. Deactivation of Pt-CeO_2 catalysts used in realistic WGS streams [10] and in start–stop operation [11] has also been reported. Alternatives to platinum are desirable in order to overcome these problems, and importantly, to reduce the high cost associated with platinum-based catalysts.

* Corresponding author. Tel.: +1 617 627 3048; fax: +1 617 627 3991.
E-mail address: mflytzan@tufts.edu (M. Flytzani-Stephanopoulos).

0926-860X/$ – see front matter © 2005 Elsevier B.V. All rights reserved.
doi:10.1016/j.apcata.2005.02.048

In recent years, nanostructured gold catalysts have attracted interest as potential candidates for CO removal processes. This was prompted by Haruta's reports of very high activity of gold nanoparticles on reducible oxide supports for the CO oxidation reaction [12,13]. Gold-iron oxide catalysts have been shown to be more selective for the CO oxidation reaction compared to platinum group catalysts [13–17]. Other nanoscale gold-oxide systems evaluated in the recent literature as PROX catalysts include Au-Al_2O_3 [18,19], Au-TiO_2 [20,21], Au-ZnO [22], Au-Co_3O_4 and SnO_2 [21], and Au-CeO_2 [21,23–27].

Nanostructured gold-ceria oxidation catalysts have certain unique properties for low-temperature reformate gas processing. Gold-ceria was first evaluated as a CO oxidation catalyst by Gardner et al. [28] and then Liu and Flytzani-Stephanopoulos [29,30]. Weber found that the preparation conditions affected the CO oxidation properties and stability of gold-ceria [31]. Fu et al. was the first to report on the excellent WGS activity of gold-ceria [32], and to identify the importance of the cerium oxide structure for the WGS activity of this catalyst [32–36]. Since 2002, other groups have reported similar findings [37–43].

We recently found that only gold strongly bound to ceria participates in the WGS catalysis [34–36]. Metallic gold nanoparticles are merely spectator species. The amount of gold that remains in ceria after leaching in a sodium cyanide solution is dictated by the surface properties of ceria [34–36], and it is in the form of gold cations. In this paper, we examine whether low-content gold-ceria samples are also active and stable in the PROX reaction in realistic fuel gas mixtures.

2. Experimental

2.1. Catalyst preparation and characterization

Lanthana- or gadolinia-doped ceria and undoped ceria materials were prepared by the urea gelation/co-precipitation (UGC) method [44], as adapted for ceria materials by Kundakovic and Flytzani-Stephanopoulos [45]. Low-content gold-ceria samples were prepared by the UGC method, and by deposition–precipitation (DP) followed by leaching in a NaCN solution at pH 12 to remove weakly bound gold. Details about the preparation techniques can be found elsewhere [34–36]. Cyanide leaching removed ~90% of the gold from the parent gold-ceria samples, but no other component was leached out, as checked by ICP. Leached samples were washed with deionized water three times; then, dried in a vacuum oven for 10 h and heated in air at 400 °C for 2 h.

All reagents used in catalyst preparation were analytical grade. The samples reported here are denoted as *a*AuCeLa or CeGd (*z*), where *a* is the gold content in atomic percent $100 \times (\mathrm{Au/MW_{Au}})/(\mathrm{Au/MW_{Au}} + \mathrm{Ce/MW_{Ce}} + \mathrm{La}$ or $\mathrm{Gd/MW_{La\ or\ Gd}})$, CeLa is 10 at.% La-doped ceria, CeGd is 10 at.% Gd-doped ceria, and *z* is the method of gold addition: DP or UGC. The calcination temperature was typically 400 °C.

The BET surface area was measured by single-point N_2 adsorption/desorption cycles in a Micromeritics Pulse ChemiSorb 2705 flow apparatus. Bulk composition analysis of the catalyst was conducted in an Inductively Coupled Plasma Optical Emission Spectrometer (ICP-OES, Leeman Labs Inc.).

A Kratos AXIS Ultra Imaging X-ray Photoelectron Spectrometer with a resolution of 0.1 eV was used to determine the atomic metal ratios of the surface region and the oxidation state of gold in selected catalysts. Samples in powder form were pressed on a double-side adhesive copper tape for analysis. All measurements were carried out at room temperature without any sample pre-treatment. An Al Kα X-ray source was used in this work. All binding energies were adjusted to the C1s peaks at 285 eV. The instrument is calibrated using Au foil at 83.8 eV. An adjacent neutralizer was used to minimize the static charge on the samples.

Scanning transmission electron microscopy (STEM) analyses were performed in a Vacuum Generator HB603 STEM instrument equipped with an X-ray microprobe of 0.14 nm optimum resolution for Energy Dispersive X-ray Spectroscopy (EDX). The sample powder was dispersed on a copper grid coated with a carbon film and elemental maps were obtained on a 128 × 128 data matrix.

XRD analysis was performed on a Rigaku 300 instrument with a rotating anode generator and a monochromatic detector. Cu $K\alpha_1$ radiation was used with a power setting of 60 kV and 300 mA. Typically, a scan rate of 2°/min with 0.02° data interval was used. Tungsten was used as an internal standard. The software TOPAS (Bruker) was used to perform microstructure analysis.

2.2. Apparatus and experimental procedures

Temperature-programmed reduction by hydrogen (H_2-TPR) was conducted in a Micromeritics Pulse ChemiSorb 2705 instrument equipped with a thermal conductivity detector to detect H_2 consumption. The as-prepared catalysts in fine powder form were heated at a rate of 5 °C/min from room temperature to 400 °C in a 20% H_2/N_2 (50 cm^3/min (NTP)).

WGS reaction and PROX reaction tests were conducted at atmospheric pressure with the catalyst in powder form (<150 μm). A quartz tube (o.d. = 1 or 0.5 cm) with a porous quartz frit supporting the catalyst was used as a packed-bed flow reactor. Water was injected into the flowing gas stream by a calibrated syringe pump and vaporized in the heated gas feed line before entering the reactor. A condenser filled with ice was installed at the reactor exit to collect water. The feed and product gas streams were analyzed by a HP-6890 gas chromatograph (GC) equipped with a thermal conductivity detector (TCD). A Carbosphere (Alltech) packed column (6 ft × 1/8 in.) was used to separate O_2, CO, H_2, and CO_2.

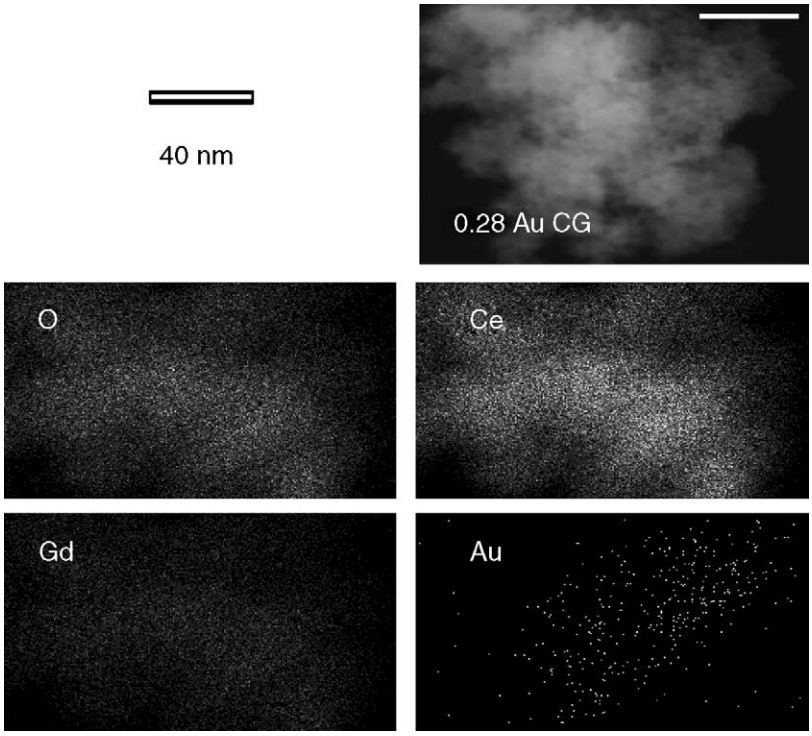

Fig. 1. STEM/EDX of as-prepared 0.28AuCeGd (UGC), see Table 1 for properties.

No methane was produced under any of the operating conditions used in this work.

The molar feed gas composition used for WGS was 11% CO–26% H_2O–26% H_2–7% CO_2–He. The total gas flow rate of the reactants was kept constant at 207 mL/min. The percent CO conversion (X_{CO}) is determined by:

$$X_{CO}\,(\%) = 100 \times \frac{CO_{in} - CO_{out}}{CO_{in}}$$

The feed gas for PROX is composed of 1% CO–0.5% O_2–10% H_2O–50% H_2–15% CO_2–He. The total flow rate of the reactants was kept constant at 125 mL/min. The percent CO conversion (X_{CO}) is calculated as above, while the percent selectivity to CO oxidation is defined as:

$$S_{CO}\,(\%) = 100\frac{0.5(CO_{in} - CO_{out})}{(O_2)_{in} - (O_2)_{out}}$$

3. Results and discussion

3.1. Sample characterization

Low-content gold-ceria catalysts prepared by basic sodium cyanide leaching of parent gold-ceria samples, themselves prepared by deposition–precipitation, showed no metallic gold remaining, as confirmed by STEM/EDX and XPS [34–36]. The activities of the leached samples for the WGS reaction were the same or a little higher than the parent catalysts, which contained ~10 times more gold, mostly as metallic gold nanoparticles [34]. A 0.57AuCeLa (DP, NaCN) was prepared in this way by removing the weakly bound gold from 5.8AuCeLa (DP). If low-content gold-ceria catalysts with atomically dispersed gold can be prepared by a one-pot method, this would simplify the catalyst preparation process. In this work, 0.28AuCeGd (UGC) was synthesized directly by the UGC method. HRTEM showed no gold particles present, while the Gd-doped ceria was nanocrystalline with a mean particle size of 5.8 nm. Fig. 1 shows elemental maps for O, Ce, Gd, and Au obtained from STEM/EDX analysis of 0.28AuCeGd (UGC). Au

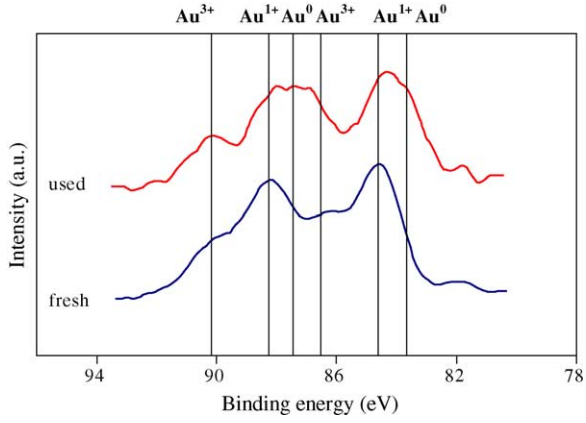

Fig. 2. XP spectra of Au_{4f} in as-prepared and used 0.28AuCeGd (UGC) after 50 h in PROX reaction at 120 °C, 1% CO–0.5% O_2–50% H_2–10% H_2O–15% CO_2–balance He.

Table 1
Physical properties of gold-ceria materials[a]

Sample	BET S.A. (m^2/g)	Bulk composition[b] (at.%)			Crystallite size[c] (nm)		
		Au	Ce	La or Gd	Au	CeO_2	
					⟨1 1 1⟩	⟨1 1 1⟩	⟨2 2 0⟩
5.8AuCL (DP)	164.9	5.83	86.48	7.68	4.5	6.0	7.1
0.57AuCL (DP, NaCN)	160.9	0.57	92.03	7.40	ND	5.6	6.8
0.28AuCG (UGC)	158.2	0.28	90.62	9.10	ND	5.4	6.1
1.41AuCG (UGC)	159.5	1.41	90.40	8.19	ND	4.9	6.1
4.6AuCL (DP)	153.0	4.60	87.50	7.90	NM	NM	NM
0.2AuCL (DP, NaCN)	156.0	0.20	91.30	8.50	NM	NM	NM
0.69$AuCeO_2$ (UGC)	170.1	0.69	99.31	–	ND	5.0	6.2
0.94$AuCeO_2$ (UGC)	180.5	0.94	99.06	–	ND	4.3	5.4
CeGd (UGC)	173.2	0	89.81	10.19	–	5.0	6.3
CeLa (UGC)	156.9	0	92.62	7.38	–	5.1	4.8
CeO_2 (UGC)	140.5	–	100.00	–	–	7.1	6.6

ND, non detectable; NM, not measured.
[a] All samples calcined at 400 °C in air for 10h, except the leached samples for 2h; CeLa: Ce(10% La)O_x; CeGd: Ce(10% Gd)O_x calcined at 400 °C, 10 h.
[b] Bulk composition was determined by Inductively Coupled Plasma (ICP) emission spectrometry.
[c] The crystallite size was determined from XRD data with the Scherrer equation.

appears to be atomically dispersed in the Gd-doped ceria matrix. Only cationic gold was found by XPS as shown in Fig. 2. The binding energies for the as-prepared catalyst correspond to Au^{1+} (84.6 and 88.2 eV) and Au^{3+} (86.5 and 90.1 eV) [34,46,47]. The physical properties of the catalysts examined in this work are shown in Table 1.

The UGC-prepared gold-ceria samples have a smaller ceria particle size compared to gold-free ceria prepared by the same method, as shown in Table 1. For example, in the samples containing 0.69 and 0.94 at.% Au in ceria, the particle size of ceria (1 1 1) is 5 and 4.3 nm, respectively, i.e. much smaller than the 7.1 nm particle size of gold-free ceria (Table 1). If Au^{3+} ions with radius 0.099 nm [48] substitute into the ceria lattice, this should be accompanied by an increase of the value of the lattice constant. The lattice constants of gold-free ceria and the gold-ceria samples prepared by UGC under the same conditions are shown in Fig. 3a. Clearly, a considerable lattice expansion is seen in the gold-ceria samples. At this point we cannot assign the expansion to just gold Au^{3+} ion substitution, as it is possible that some or most of the expansion is caused by the presence of Ce^{3+} in nanoscale ceria [49]. In either case, gold addition has a major effect in suppressing the crystal growth of ceria.

The presence of ionic gold in ceria was also examined by H_2-TPR. Fig. 3b shows the H_2-TPR profiles of 0.69$AuCeO_2$ (UGC) and 0.94$AuCeO_2$ (UGC). These indicate that most gold is present in oxidized form, since oxygen adsorbed on metallic gold nanoparticles has a reduction peak at a temperature below 50 °C [33], which is absent here. The reduction of 0.94$AuCeO_2$ begins at lower temperatures compared to the 0.69$AuCeO_2$ sample. However, the peak shapes and the total hydrogen consumption (1000 ± 50 $\mu mol/g_{cat}$) are similar in both samples. Leaching by a NaCN solution at pH 12 removed about 20% of the total gold from both materials. Hence, only a small amount of weakly bound gold is present in low-content gold-ceria prepared by the one-pot UGC method and calcined at 400 °C.

3.2. WGS reaction activity

We have recently reported that similar WGS reaction rates were measured over the parent and corresponding leached gold-ceria catalysts, showing that metallic gold nanoparticles do not participate in the WGS reaction [34,36]. The active site

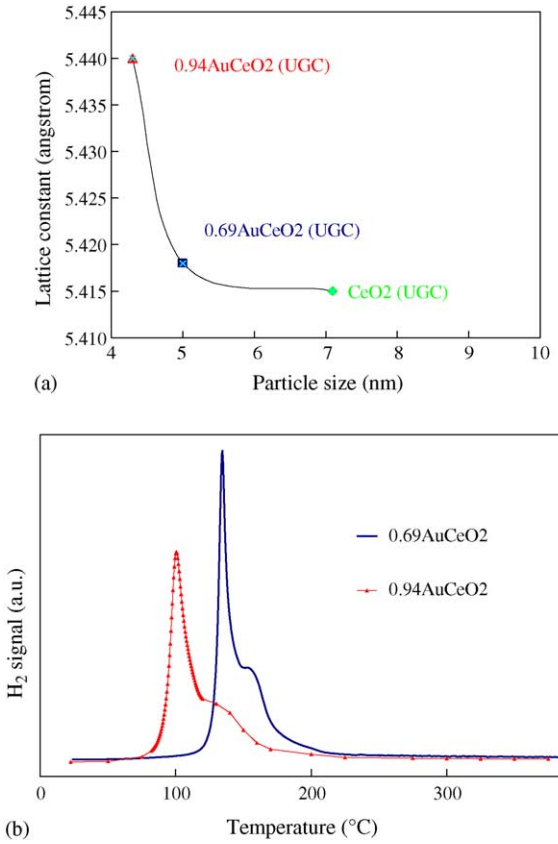

Fig. 3. (a) Lattice expansion of ceria in gold-ceria samples prepared by the UGC method; 400 °C-calcined (see Table 1) and (b) H_2-TPR profiles of gold-ceria prepared by the UGC method; 20% H_2/N_2, 50 cm^3/min (NTP), 5 °C/min; samples were purged in He at room temperature for 30 min before the TPR test.

for the WGS reaction appears to be a Au–O–Ce structure, involving atomically dispersed gold in ceria. Turnover frequencies can be calculated by scaling the rates with the amount of gold, assuming atomic dispersion for the leached samples and for the low-content gold-ceria samples prepared by one-pot UGC. As reported elsewhere [36], the TOFs thus calculated are in remarkable agreement, given the variability in sample composition and preparation. Here, we calculated a lower bound for the TOFs by normalizing the steady-state WGS reaction rates by the amount of reducible oxygen on the surface as measured by H_2-TPR. The TOF values expressed as CO_2 molecules produced/s/surface O_2 molecule, are shown in Fig. 4. These are about an order of magnitude lower than the TOFs expressed per Au atom [36]. This is a reasonable agreement since not all the surface oxygen participates in the WGS reaction; and the TPR technique is not totally surface sensitive. The apparent activation energy calculated from Fig. 4 is 49 ± 5 kJ/mol; similar to the E_a values previously reported [34,36].

3.3. PROX reaction activity

It is interesting to evaluate the activity of the low-content gold-ceria samples for the preferential CO oxidations in H_2-rich reformate gas streams. There is presently no consensus in the literature as to what the active sites of gold are for either the PROX reaction or the CO oxidation in the absence of hydrogen. Haruta et al. [13,15,16] consider metallic gold nanoparticles as indispensable for CO oxidation on gold-oxide supports. The interfacial length between the gold nanoparticles and the support is considered to be very important, so smaller particles lead to higher activity. Valden et al. found a maximum in the CO oxidation activity of gold on titania at ~3.4 nm gold particle size [50]. More recently, Bond and Thompson argued that on the basis of the then existing literature, both metallic and ionic gold sites are necessary to catalyze the CO oxidation [51]. Guzman and Gates [52] studied Au-MgO catalysts using in situ XANES

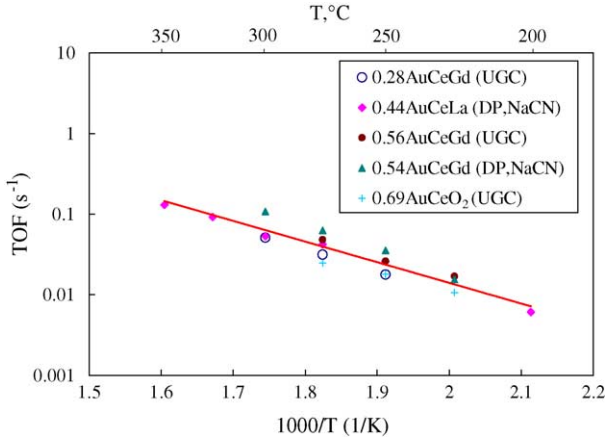

Fig. 4. Turnover frequencies (mol CO_2/s/mol surface O_2) of the WGS reaction over low-content gold-ceria catalysts in a gas mixture of 11% CO–26% H_2O–26% H_2–7% CO_2–balance He.

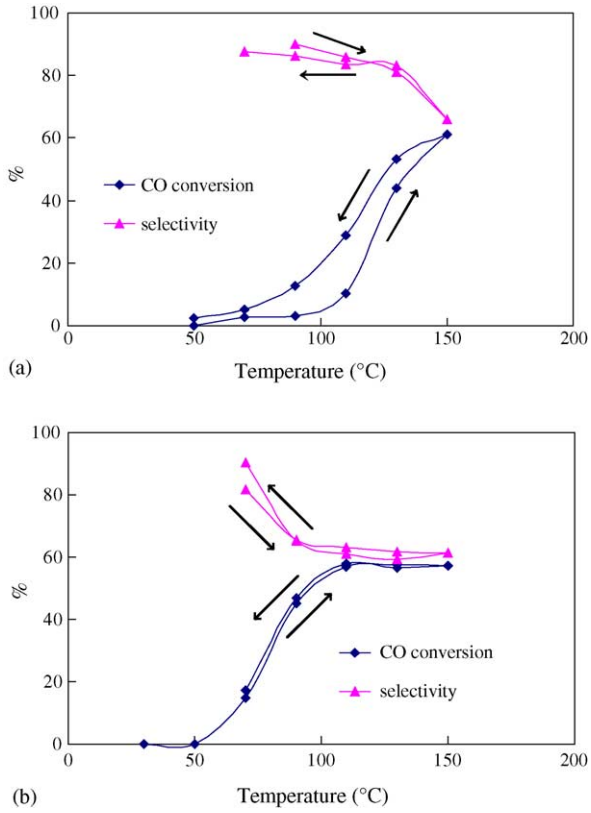

Fig. 5. CO conversion and oxygen selectivity in the PROX reaction over gold-ceria catalysts: (a) 0.28AuCeGd (UGC) and (b) 1.41AuCeGd (UGC). Gas mixture: 1% CO–0.5% O_2–50% H_2–2% H_2O–balance He; W/F = 0.0034 g s/cm^3.

and determined that during steady-state CO oxidation, the catalyst contained both Au^{1+} and Au^0 regardless of the initial oxidation state (positive or neutral) of the gold.

In this work, we evaluated the PROX activity of low-content gold-ceria catalysts. In Fig. 5, the samples 0.28AuCeGd (UGC) (Fig. 5a) and 1.41AuCeGd (UGC) (Fig. 5b) were tested in a gas mixture of 1% CO–0.5% O_2–50% H_2–2% H_2O, linearly ramping the reaction temperature from room temperature to 150 °C, and cooling back to room temperature. With increasing temperature, the CO conversion increased and the selectivity for CO oxidation decreased. The light-off temperature of H_2 oxidation is higher than that of CO oxidation on gold-ceria, as evidenced by comparison of H_2- and CO-TPR [24,25,33–36], which can explain the drop of selectivity with temperature. The CO conversion over 0.28AuCeGd (UGC) is lower than that over the 1.41AuCeGd (UGC) sample at temperatures below 130 °C, indicating that the latter contains more active sites. We found that ~70% of the gold in 1.41AuCG (UGC) is strongly bound (non-leachable) to ceria which is three times the amount of gold in 0.28AuCG (UGC). The hysteresis shown for 0.28AuCeGd (UGC) in Fig. 5a was not present in 1.41AuCeGd (UGC) in Fig. 5b. Thus, the former catalyst was activated by the reaction gas mixture.

Fig. 6 compares the H_2-TPR profiles of 0.28AuCeGd (UGC), as-prepared (400 °C air calcined) and after use in the

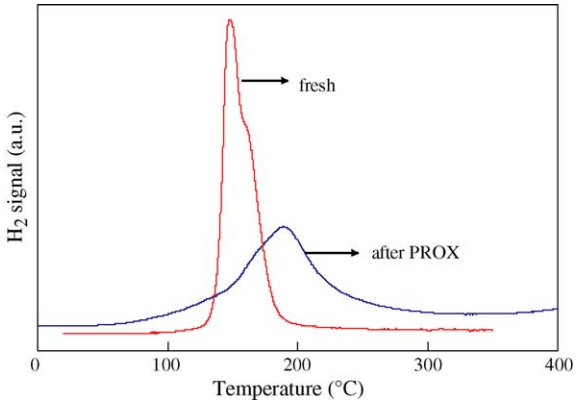

Fig. 6. H_2-TPR profiles of 0.28AuCeGd (UGC) before and after use in the PROX reaction. Samples were purged in He at room temperature for 30 min before the TPR test; 20% H_2/N_2, 50 cm^3/min (NTP), 5 °C/min; PROX condition: W/F = 0.18 g s/cm^3; 1% CO–0.5% O_2–50% H_2–2% H_2O–15% CO_2–balance He up to 120 °C for 17 h.

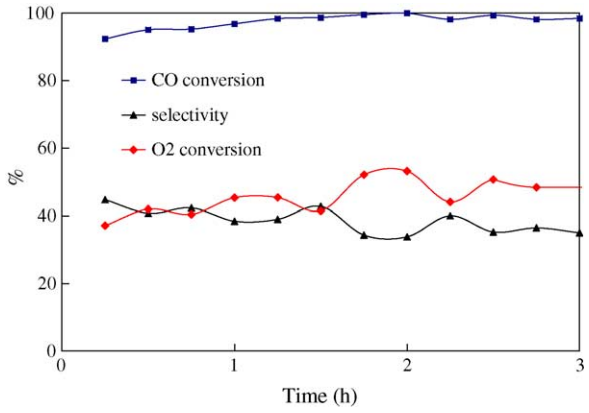

Fig. 7. CO conversion and oxygen selectivity in the PROX reaction over 0.28AuCeGd (UGC) in excess O_2; feed gas: 1% CO–2.5% O_2–50% H_2–10% H_2O–15% CO_2–He; 110 °C; W/F = 0.48 g s/cm^3.

PROX reaction up to 150 °C in a gas mixture containing (mol): 1% CO–0.5% O_2–50% H_2–2% H_2O–15% CO_2–He. The as-prepared material contains cationic gold, as also confirmed by XPS, and its reduction begins around 120 °C. After 17 h of PROX reaction, reduction of the used sample begins at ~50 °C, but the peak is broader, extending to 300 °C. The hydrogen consumption over these two samples is similar, 677 μmol/g_{cat} for the fresh sample and 680 μmol/g_{cat} for the used one. Thus, under the PROX reaction conditions, part of the catalyst changed oxidation state, but this did not result in activity loss. It is not clear at this point whether gold, cerium or both change oxidation states as a result of exposure to the reaction gas mixture. Since considerable reoxidation of the reduced gold-ceria samples takes place readily at room temperature in air (see below), in situ techniques must be used to examine the extent of sample reduction under reaction conditions.

Highly active and selective catalysts are sought for the PROX reaction to reduce the CO concentration to a level that can be tolerated by PEM fuel cells. Most tests in this work used stoichiometric amount of oxygen to oxidize CO over the gold-ceria catalysts. In the temperature range from 80 to 120 °C, less than complete CO conversion and less than 100% oxygen selectivity were obtained when using the stoichiometric oxygen to CO ratio and a high space velocity with W/F = 0.096 g s/cm^3. However, if excess O_2 is used, the target CO level can be achieved with W/F = 0.48 g s/cm^3 at 110 °C over the 0.28AuCeGd (UGC) material, as shown in Fig. 7. Approximately, 50% of the oxygen was consumed by both CO and H_2 at the conditions of Fig. 7, and the selectivity was ~40%, which implies that a low-content gold-ceria catalyst is a viable candidate for the PROX reaction. Further investigation is warranted to examine the effect of the experimental parameters on catalyst activity and selectivity.

The rates of CO oxidation over the gold-ceria catalysts were measured from 30 to 140 °C in the absence and presence of hydrogen, carbon dioxide and/or water. The sample 4.6AuCeLa (DP) was found to be about four times more active than 0.2AuCeLa (DP, NaCN) for CO oxidation, which is much less than the difference in gold loading (23-fold) between these two catalysts. In the full gas stream, which is composed of 1% CO–0.5% CO_2–50% H_2–2% H_2O–15% CO_2–He, the 4.6AuCeLa (DP) sample is only twice as active as the 0.2AuCeLa (DP, NaCN) sample, indicating that most of the gold present in the 4.6AuCeLa (DP) sample does not participate in the reaction [24,25].

Fig. 8 compares the turnover frequencies of the PROX reaction over the 0.2AuCeLa (DP, NaCN) and 0.28AuCeGd (UGC) samples under realistic reaction conditions. The TOF is calculated by scaling the rate with the amount of gold, which assumes that all gold is fully exposed in these samples. A very good agreement is seen for the two very differently prepared samples. We did not include data for 4.6AuCeLa (DP) in Fig. 8, because some gold is present as metallic nanoparticles in that sample. Comparison of Figs. 4 and 8 reveals the much higher activity of the gold-ceria catalysts for the PROX than the WGS reaction.

3.4. Reversibility in redox gas treatment

Cyclic H_2-TPR was conducted to determine the reversibility of gold-ceria structures in redox treatment. It has

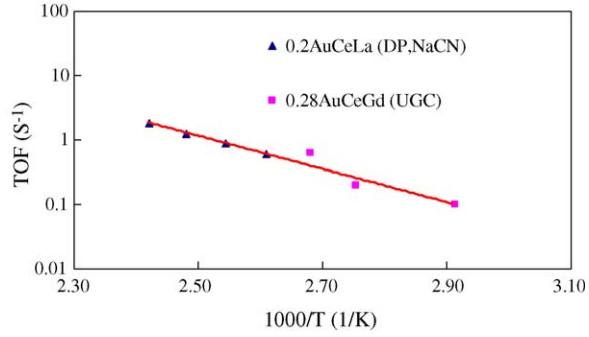

Fig. 8. TOF of the PROX reaction over low-content gold-ceria catalysts prepared by different methods. Feed gas: 1% CO–0.5% O_2–50% H_2–2% H_2O–15% CO_2–He; W/F = 0.0034 g s/cm^3.

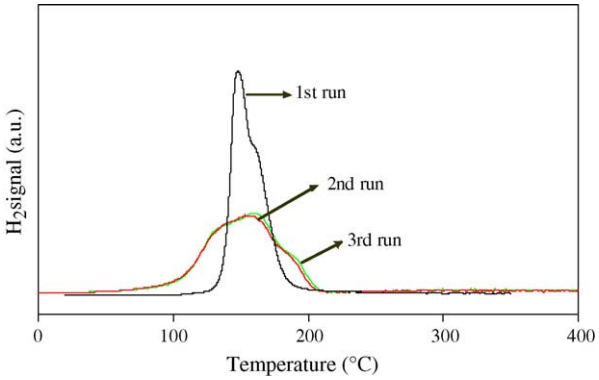

Fig. 9. Cyclic H_2-TPR profiles of 0.28AuCeGd (UGC); 20% H_2/N_2; 50 cm^3/min (NTP); after each run, the sample was oxidized in a stream of 20% O_2/He at 350 °C for 30 min, then purged in He at room temperature for 30 min.

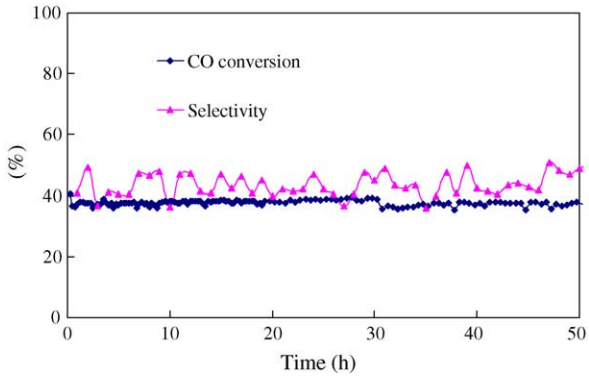

Fig. 10. Stability of 0.28AuCeGd (UGC) catalyst in the PROX reaction for 50 h at 120 °C. W/F = 0.096 g s/cm^3; feed gas mixture: 1% CO–0.5% O_2–50% H_2–10% H_2O–15% CO_2–balance He.

been reported that irreversible changes occur to Au/Fe_2O_3 [53] and Au/TiO_2 [54] after reduction, which might explain the deactivation of these catalysts. On the other hand, gold-ceria structures are reversible in cyclic CO-TPR with intermittent reoxidation [35,36]. Here, we report on the reversibility of gold-ceria structures in various gas mixtures and temperatures. Three cycles of H_2-TPR are shown in Fig. 9. The sample 0.28AuCeGd (UGC) was reduced in 20% H_2/N_2 up to 400 °C, and then reoxidized in 20% O_2/He at 350 °C for 30 min. After purging in He for 30 min, the cycle was repeated. The H_2 consumption for the first, second and third run was 677, 572, and 585 $\mu mol/g_{cat}$, respectively. During the first reduction by hydrogen up to 400 °C, some irreversible surface change occurs, as indicated by some loss of oxygen in subsequent cycles. However, after the second cycle total reversibility is observed. Similar results were also found in cyclic H_2-TPR of 0.57AuCeLa, prepared from 5.8AuCeLa (DP) by sodium cyanide leaching. Thus, the surface structures of gold-ceria catalysts are highly reducible and they can be reoxidized by O_2.

Further, we examined the effect of other oxidants and temperatures on the oxidation state and reversibility of gold-ceria surfaces. The sample 0.57AuCeLa (DP, NaCN) was first reduced in a 20% H_2/N_2 gas stream in the TPR mode up to 400 °C (with consumption of H_2 amounting to ~650 $\mu mol/g_{cat}$), and then reoxidized under various conditions as shown in Table 2. The subsequent sample reducibility was checked again by H_2-TPR. We found that reoxidation of the reduced gold-ceria samples took place readily at room temperature by O_2, H_2O or air, but not by CO_2. Room temperature reoxidation by oxygen has also been reported by Andreeva et al. [37]. Importantly, we report here for the first time that H_2O can also reoxidize the gold-ceria surface at room temperature. Thus, under WGS reaction conditions, H_2O would be the relevant oxidizer. However, only around one-third of the oxygen capacity can be restored at room temperature. At higher temperatures (350 °C) in oxygen, as shown in Fig. 9 and Table 2, recovery is complete. These findings, especially the reoxidation of the surface by water vapor at room temperature, are important in structural and mechanistic interpretations of this type catalyst. The gold-ceria surface is under a dynamic oxidation state, determined not only by the total reducing quality of the gas, but also by the type of oxidant present.

3.5. Gold-ceria stability in realistic PROX reaction gas streams

Long-term tests with the 0.28AuCeGd (UGC) catalyst were conducted to evaluate the catalyst stability under

Table 2
Reversibility of 0.57AuCeLa (DP, NaCN) surface in redox treatments[a]

Oxidized by	Temperature (°C)	Purged by	H_2-TPR (RT to 400 °C, 5 °C/min)	
			H_2 consumption ($\mu mol/g$)	Peak temperature (°C)
He	RT	He	0	N/A
20% O_2	RT	He	215	112.8
Air	RT	He	188	114.5
3% H_2O	RT	He	235	120.5
100% CO_2	RT	He	0	N/A
100% CO_2	350	He	0	NA
3% H_2O + 97% CO_2	350	He	297	127.5
20% O_2	350	He	572	120.3

[a] Samples were first reduced in a 20% H_2/N_2 gas stream from RT to 400 °C at a heating rate of 5 °C/min, then oxidized by different gases at different temperatures for 30 min and purged in He at room temperature for 30 min before a second H_2-TPR test at the same conditions as above.

Table 3
Properties of 0.28AuCeGd (UGC) before and after the PROX reaction[a]

Sample	BET S.A. (m^2/g)	Bulk Au content [b] (at.%)	Surface Au content [c] (at.%)	CeO_2 crystallite size[d] (nm)		Hydrogen consumption[e] (μmol/g_{cat})	TOF at 70 °C (s^{-1})[f]
				⟨1 1 1⟩	⟨2 2 0⟩		
Fresh	158.2	0.28	0.20	5.4	6.1	677	0.143
Used after PROX[a]	153.0	0.20[g]	0.12	5.7	6.3	680[h]	0.145

[a] PROX condition: 1% CO–0.5% O_2–50% H_2–10% H_2O–15% CO_2–He; temperature: 120 °C; 50 h.
[b] Bulk composition was determined by Inductively Coupled Plasma (ICP).
[c] The surface metal content was determined by XPS.
[d] Crystallite size was determined by XRD with the Scherrer equation.
[e] Hydrogen consumption was measured by H_2-TPR from RT to 400 °C, samples were purged with He at RT before testing.
[f] The turnover frequencies were calculated by normalizing rates by the surface gold content, test condition: 1% CO–0.5% O_2–50% H_2–2% H_2O–15% CO_2–He.
[g] The used sample was leached with NaCN solution (pH 12).
[h] PROX reaction condition: 1% CO–0.5% O_2–50% H_2–2%H_2O–15% CO_2–He; temperature up to 120 °C for 17 h.

PROX reaction conditions. The feed gas mixture contained 1% CO–0.5% O_2–50% H_2–15% CO_2–10% H_2O–He. The reaction was run for 50 h at 120 °C. Fig. 10 shows that there was no loss of CO oxidation activity or oxygen selectivity over the time period tested. Similar results have been reported for Au/α-Fe_2O_3, which did not deactivate after 70 h on stream at 100 °C in selective CO oxidation in the presence of 15% CO_2 and 10% H_2O [14].

The 50-h used 0.28AuCeGd (UGC) sample was analyzed by XPS. Binding energies of Au 4f are shown in Fig. 2. A part of gold remained ionic, while some zerovalent gold is also present (binding energies of 83.8 and 87.4 eV). Deconvolution of the spectra shows that the zerovalent species amount to 34.9% of the total gold present in the 0.28AuCeGd (UGC) sample. We attribute the partial reduction of gold to the reaction conditions, and not to the X-ray beam, because the latter had no effect on the fresh sample (all ionic gold) also shown in Fig. 2.

No deactivation was observed over any of the gold-ceria catalysts used in the PROX reaction in this work, which probably means that the surface structure adapts to the gas composition very quickly, within the first few minutes on stream.

XRD analysis found no appreciable difference between the fresh and used 0.28AuCeGd (UGC) samples with respect to the crystallite size of ceria. As shown in Table 3, the mean particle size of ceria is 5.8 nm for the fresh material and 6.0 nm for the one used in the PROX reaction at 120 °C for 50 h. The BET surface area is 158.2 m^2/g for the as-prepared material and 153.0 m^2/g for the used one. By XPS analysis, the surface gold content was found to have dropped from 0.20 to 0.12 at.%. If we compare the turnover frequencies normalized by the surface amount of gold in the fresh and used materials, the activity scales with the surface gold content (see Table 3, at 70 °C).

3.6. Carbonate issues

Cerium carbonate formation has been reported at low temperatures [7]. In the literature, deactivation of Au–metal oxide catalysts for the CO oxidation reaction is mostly attributed to the accumulation of carbonate species, which can block active sites [17,21]. The formation of carbonates can occur by the adsorption of CO_2 in air as shown on as-prepared Pt/CeO_2 [11] or from CO_2 present in the reactant or product gas mixture. Fig. 11 shows the PROX performance of 4.6AuCeLa (DP) upon addition of 15% CO_2 to the feed gas mixture. Region A shows that at 70 °C and a contact time of 0.0017 g s/cm^3, about 10% CO conversion and 60% oxygen selectivity are achieved. After CO_2 is added (Region B), the CO conversion drops to almost zero. However, when CO_2 is removed from the feed, the CO conversion, as well as selectivity, is restored. Interestingly, in the presence of CO_2 and H_2O together no deactivation of 0.28AuCeGd (UGC) was observed. Under realistic conditions, water will be present in the feed gas to the PROX reactor. The water effect alone was found to enhance the PROX activity, as shown for the low-content 0.28AuCeGd (UGC) sample in Fig. 12. After steady state was reached in the gas mixture of 1% CO–0.5% O_2–50% H_2–15% CO_2–He for 10 h at 120 °C, 10% H_2O was introduced into the reactor and a CO conversion jump was observed. When H_2O was removed from the stream, the CO conversion dropped back to the initial level. The same

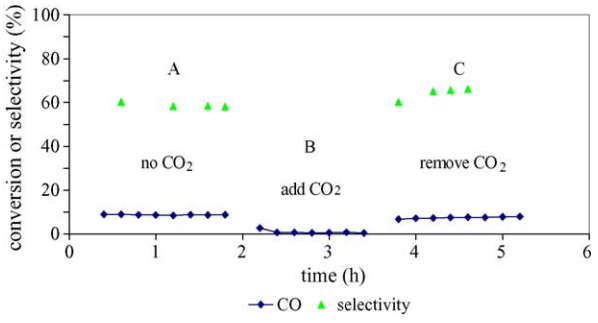

Fig. 11. Effect of CO_2 on the CO conversion and oxygen selectivity in the PROX reaction over 4.6AuCeLa (DP); feed gas: 1% CO–0.5% O_2–68% H_2–2% H_2O–balance He; W/F = 0.0017 g s/cm^3; T = 70 °C. Regions A and C are for no CO_2 in the feed gas. In region B, 15% CO_2 was added.

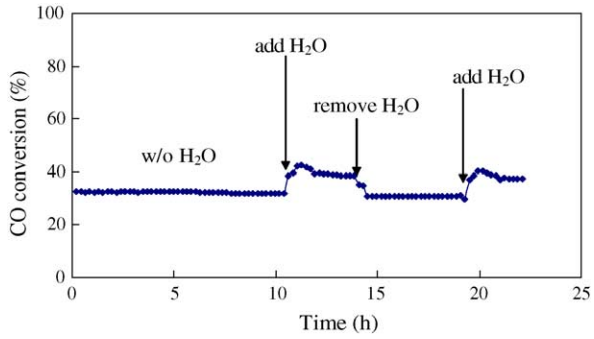

Fig. 12. H_2O enhancement of the PROX reaction over 0.28AuCeGd (UGC) at 120 °C. W/F = 0.096 g s/cm^3; 1% CO–0.5% O_2–50% H_2–0 or 10% H_2O–15% CO_2–balance He.

response was observed when H_2O was again introduced in the feed gas stream. In the literature, on other gold catalysts for the PROX reaction, there are reports that addition of H_2O can prevent the deactivation of Au/α-Fe_2O_3 [17] and Au/Al_2O_3 [19] and may enhance the rate of decomposition of carbonate species by reactive conversion to bicarbonate species, which are thermally less stable. A similar examination of Au-CeO_2 PROX catalysts is not presently available. However, we have found that cerium hydroxycarbonate is formed during shutdown in the full WGS gas mixture over gold-ceria catalysts; and this is detrimental to the WGS activity [36]. An examination of the stability differences of gold-ceria in the WGS and PROX reactions is the subject of a future report.

4. Conclusions

One-pot UGC synthesis of low-content (<0.6 at.%) gold-ceria catalysts produces very highly dispersed gold in ceria, after 400 °C calcination in air. Gold cations are present in the as-prepared catalysts; partial substitution of Au^{3+} in the ceria lattice is a plausible explanation for the measured suppression of the crystal growth of ceria. These materials have similar activity in the WGS and PROX reactions to low-content gold-ceria samples prepared by cyanide leaching of parent catalysts. The surface structures of gold-ceria materials are highly reversible in cyclic redox conditions. Partial reoxidation of a catalyst reduced at 400 °C occurs even at ambient conditions. Oxygen, water, but not carbon dioxide, can be used as oxidants. While CO_2 is found to suppress the rate of the PROX reaction, gold-ceria catalysts have remarkable stability in realistic PROX gas mixtures over a wide range of temperatures.

Very little gold is needed to activate the surface oxygen of ceria, and most of it remains ionic even after prolonged reaction at 120 °C. Similar to the WGS reaction, strongly bound gold in ceria appears to be involved in catalyzing the PROX reaction. Complementary in situ techniques should be used to study the extent of reduction of gold and cerium oxide species in either reaction, identify the relevant catalytic sites, and guide further catalyst design and development.

Acknowledgements

The financial support of this work by the NSF/EPA, Grant # CTS-9985305 and by the NSF Nanoscale Interdisciplinary Research Team (NIRT) Grant # 0304515, is gratefully acknowledged. We thank Anthony Garratt-Reed and Elisabeth Shaw of MIT for their assistance with the STEM/EDX and XPS analyses.

References

[1] D.S. Newsome, Catal. Rev. Sci. Eng. 21 (1980) 275.
[2] S.H. Oh, R.M. Sinkevitch, J. Catal. 142 (1993) 254.
[3] C. Plog, W. Maunz, T. Stengel, R. Andorf, Eur. Patent 0,650,922,A1 (1995).
[4] M.J. Kahlich, H.A. Gasteiger, R.J. Behm, J. Catal. 171 (1997) 93.
[5] A. Manasilp, E. Gulari, Appl. Catal. B: Environ. 37 (2002) 17.
[6] T. Bunluesin, R.J. Gorte, G.W. Graham, Appl. Catal. B: Environ. 15 (1998) 107.
[7] S. Hilaire, X. Wang, T. Luo, R.J. Gorte, J. Wagner, Appl. Catal. A: Gen. 215 (2001) 271.
[8] S.L. Swartz, M.M. Seabaugh, C.T. Holt, W.J. Dawson, Fuel Cell Bull. 30 (2001) 7.
[9] F. Marino, C. Descorme, D. Duprez, Appl. Catal. B: Environ. 54 (2004) 59–66.
[10] J.M. Zalc, V. Sokolovskii, D.G. Loffler, J. Catal. 206 (2002) 169.
[11] X. Liu, W. Ruettinger, X. Xu, R. Farrauto, Appl. Catal. B: Environ. 56 (2005) 69–75.
[12] M. Haruta, N. Yamada, T. Kobayashi, S. Iijima, J. Catal. 115 (1989) 301.
[13] M. Haruta, S. Tsubota, T. Kobayashi, H. Kageyama, M. Genet, B. Delmon, J. Catal. 144 (1993) 175.
[14] G. Avgouropoulos, T. Ioannides, Ch. Papadopoulou, J. Batista, S. Hocevar, H.K. Matralis, Catal. Today 75 (2002) 157.
[15] M. Haruta, A. Ueda, S. Tsubota, R.M. Torres Sanchez, Catal. Today 29 (1996) 443.
[16] R.M. Torres Sanchez, A. Ueda, K. Tanaka, M. Haruta, J. Catal. 168 (1997) 125.
[17] M.M. Schubert, A. Venugopal, J.J. Kahlich, V. Plzak, R.J. Behm, J. Catal. 222 (1) (2004) 32.
[18] G.K. Bethke, H.H. Kung, Appl. Catal. A: Gen. 194 (2000) 43.
[19] C.K. Costello, H.Y. Yang, Y. Wang, J.-N. Lin, L.D. Marks, M.C. Kung, H.H. Kung, Appl. Catal. A: Gen. 243 (2003) 15.
[20] B. Schumacher, Y. Denkwitz, V. Plzak, M. Kinne, R.J. Behm, J. Catal. 224 (2004) 449–462.
[21] M. Schubert, V. Plzak, J. Garche, R.J. Behm, Catal. Lett. 76 (3–4) (2001) 143.
[22] M. Manzoli, A. Chiorino, F. Boccuzzi, Appl. Catal. B: Environ. 52 (2004) 259–266.
[23] O. Goerke, P. Pfeifer, K. Schubert, Appl. Catal. A: Gen. 263 (2004) 11–18.
[24] J. De Jesus, Q. Fu, H. Saltsburg, M. Flytzani-Stephanopoulos, Annual AIChE Mtg. Paper #513b, San Francisco, CA, 16–21 November 2003.
[25] J. De Jesus, M.S. Thesis, Department of Chemical and Biological Engineering, Tufts University, 2004.
[26] G. Panzera, V. Modafferi, S. Candamano, A. Donato, F. Frusteri, P.L. Antonucci, J. Power Sources 135 (1–2) (2004) 177–183.

[27] A. Luengnaruemitchai, S. Osuwan, E. Gulari, Int. J. Hydrogen Energy 29 (4) (2004) 429–435.
[28] S. Gardner, G. Hoflund, D. Schryer, J. Schryer, B. Upchurch, E. Kielin, Langmuir 7 (1991) 2135.
[29] W. Liu, M. Flytzani-Stephanopoulos, J. Catal. 153 (1995) 304.
[30] W. Liu, M. Flytzani-Stephanopoulos, J. Catal. 153 (1995) 317.
[31] A. Weber, M.S. Thesis, Department of Chemical and Biological Engineering, Tufts University, 1999.
[32] Q. Fu, A. Weber, M. Flytzani-Stephanopoulos, Catal. Lett. 77 (1–3) (2001) 87.
[33] Q. Fu, S. Kudriavtseva, H. Saltsburg, M. Flytzani-Stephanopoulos, Chem. Eng. J. 93 (2003) 41.
[34] Q. Fu, H. Saltsburg, M. Flytzani-Stephanopoulos, Science 301 (2003) 935, published online 3 July 2003, doi: 10.1126/science.1085721.
[35] Q. Fu, Ph.D. Dissertation, Department of Chemical and Biological Engineering, Tufts University, 2004.
[36] Q. Fu, W. Deng, H. Saltsburg, M. Flytzani-Stephanopoulos, Appl. Catal. B: Environ. 56 (2005) 57–68.
[37] D. Andreeva, V. Idakiev, T. Tabakova, L. Ilieva, P. Falaras, A. Bourlinos, A. Travlos, Catal. Today 72 (1–2) (2002) 51–57.
[38] T. Tabakova, F. Boccuzzi, M. Manzoli, D. Andreeva, Appl. Catal. A: Gen. 252 (2) (2003) 385–397.
[39] A. Luengnaruemitchai, S. Osuwan, E. Gulari, Catal. Commun. 4 (5) (2003) 215–221.
[40] C.H. Kim, L. Thompson, Preprints of Symposia, American Chemical Society, Division of Fuel Chemistry, vol. 48 (1), 2003, pp. 233–234.
[41] T. Tabakova, F. Boccuzzi, M. Manzoli, J.W. Sobczak, V. Idakiev, D. Andreeva, Appl. Catal. B: Environ. 49 (2004) 73–81.
[42] H. Sakurai, S. Tsubota, M. Haruta, Catal. Catal., 44 (2002) 416–418 (as 90th CATSJ Meeting Abstracts No.2A05 published from Catalysis Society of Japan).
[43] S. Carrettin, P. Concepcion, A. Corma, J.M. Lopez Nieto, V.F. Puentes, Angew. Chem. Int. 43 (2004) 2538.
[44] Y. Amenomiya, A. Emesh, K. Oliver, G. Pleizer, in: M. Philips, M. Ternan (Eds.), Proceedings of the Ninth International Congress on Catalysis, Chemical Institute of Canada, Ottawa, 1988, p. 634.
[45] L. Kundakovic, M. Flytzani-Stephanopoulos, J. Catal. 179 (1998) 203.
[46] J.F. Moulder, W.F. Stickle, P.E. Sobol, K.D. Bomben, in: MN. Eden Prairie (Ed.), Handbook of X-ray Photoelectron Spectroscopy, Physical Electronics, Inc., 1995.
[47] J. Radnik, C. Mohr, P. Claus, Phys. Chem. Chem. Phys. 5 (1) (2003) 172.
[48] L. Minervini, M.O. Zacate, R.W. Grimes, Solid State Ionics 116 (1999) 339.
[49] F. Zhang, P. Wang, J. Koberstein, S. Khalid, Siu-Wai Chan, Surf. Sci. 563 (1–3) (2004) 74–82.
[50] M. Valden, X. Lai, D.W. Goodman, Science 281 (1998) 1647.
[51] G.C. Bond, D.T. Thompson, Gold Bull. 33 (2) (2000) 41.
[52] J. Guzman, B.C. Gates, J. Phys. Chem. B. 106 (2002) 7659.
[53] S. Minicò, S. Scirè, C. Crisafulli, A.M. Visco, S. Galvagno, Catal. Lett. 47 (1997) 273.
[54] V. Schwartz, D.R. Mullins, W. Yan, B. Chen, S. Dai, S.H. Overbury, J. Phys. Chem. B, doi: 101021/jp048076v, 2004.